

Electroweak Precision Physics from Low to High Energies *

S. HEINEMEYER[†]

Instituto de Fisica de Cantabria (CSIC-UC), Santander, Spain

Abstract

Electroweak precision observables (EWPO) can give valuable information about the last unknown parameter of the Standard Model (SM), the Higgs-boson mass M_H^{SM} . EWPO can also restrict the parameter space of new physics models (NPM) such as the Minimal Supersymmetric Standard Model (MSSM). We review the respective constraints from the W boson mass, the effective leptonic mixing angle, the anomalous magnetic moment of the muon and electric dipole moments. Within the MSSM also the lightest Higgs-boson mass, M_h , is discussed as a precision observable. The EWPO, supplemented with B physics observables and astrophysical data can be used to determine indirectly the preferred mass scales of Supersymmetry and M_h .

*plenary talk given at the *Lepton Photon 07*, August 2007, Daegu, Korea

[†]email: Sven.Heinemeyer@cern.ch

Electroweak Precision Physics from Low to High Energies

S. Heinemeyer^a

^a Instituto de Fisica de Cantabria (CSIC-UC), Santander, Spain

Electroweak precision observables (EWPO) can give valuable information about the last unknown parameter of the Standard Model (SM), the Higgs-boson mass M_H^{SM} . EWPO can also restrict the parameter space of new physics models (NPM) such as the Minimal Supersymmetric Standard Model (MSSM). We review the respective constraints from the W boson mass, the effective leptonic mixing angle, the anomalous magnetic moment of the muon and electric dipole moments. Within the MSSM also the lightest Higgs-boson mass, M_h , is discussed as a precision observable. The EWPO, supplemented with B physics observables and astrophysical data can be used to determine indirectly the preferred mass scales of Supersymmetry and M_h .

1. Introduction

The Standard Model (SM) [1] cannot be the ultimate theory of particle physics. While describing direct experimental data reasonably well, it fails to include gravity, it does not provide cold dark matter, and it has no solution to the hierarchy problem, i.e. it does not have an explanation for a Higgs-boson mass at the electroweak scale. On wider grounds, the SM does not have an explanation for the three generations of fermions or their huge mass hierarchies. In order to overcome (at least some of) the above problems, many new physics models (NPM) have been proposed in the last decades [2–5].

Theories based on Supersymmetry (SUSY) [2] are widely considered as the theoretically most appealing extension of the SM. They are consistent with the approximate unification of the gauge coupling constants at the GUT scale and provide a way to cancel the quadratic divergences in the Higgs sector hence stabilizing the huge hierarchy between the GUT and the Fermi scales. Furthermore, in SUSY theories the breaking of the electroweak symmetry is naturally induced at the Fermi scale, and the lightest supersymmetric particle can be neutral, weakly interacting and absolutely stable, providing therefore a natural solution for the dark matter problem. SUSY

predicts the existence of scalar partners \tilde{f}_L, \tilde{f}_R to each SM chiral fermion, and spin-1/2 partners to the gauge bosons and to the scalar Higgs bosons. The Higgs sector of the Minimal Supersymmetric Standard Model (MSSM) with two scalar doublets accommodates five physical Higgs bosons. In lowest order these are the light and heavy \mathcal{CP} -even h and H , the \mathcal{CP} -odd A , and the charged Higgs bosons H^\pm . Higher-order contributions yield large corrections to the masses and couplings. They can also induce \mathcal{CP} -violation leading to mixing between h, H and A in the case of general complex SUSY breaking parameters.

Other (non-SUSY) NPM comprise Two Higgs Doublet Models (THDM) [3], little Higgs models [4], or models with (large, warped, ...) extra dimensions [5]. In specific examples given later, we will mostly focus on the MSSM. However, the MSSM should be seen as a representative for a NPM. The reader may insert her/his favorite model.

So far, the direct search for NPM particles has not been successful. One can only set lower bounds of $\mathcal{O}(100)$ GeV on their masses [6]. The search reach will be extended in various ways in the ongoing Run II at the upgraded Fermilab Tevatron [7]. The LHC [8,9] and the e^+e^- International Linear Collider (ILC) [10–12] have very good prospects for exploring

NPM at the TeV scale, which is favoured from naturalness arguments. From the interplay of both machines detailed information on many NPM can be expected in this case [13].

Besides the direct detection of NPM particles (and Higgs bosons), physics beyond the SM can also be probed by precision observables via the virtual effects of the additional particles. Observables (such as particle masses, mixing angles, asymmetries etc.) that can be predicted within a certain model and thus depend sensitively on the other model parameters constitute a test of the model on the quantum level. Various models predict different values of the same observable due to their different particle content and interactions. This permits to distinguish between e.g. the SM and a NPM via precision observables. However, this requires a very high precision of the experimental results as well as of the theoretical predictions.

The wealth of high-precision measurements carried out at LEP, SLC and the Tevatron [14,15] as well as the “Muon $g-2$ Experiment” (E821) [16] and further low-energy experiments (e.g. the search for electric dipole moments (EDM), see below) provide a powerful tool for testing the electroweak theory and probing indirect effects of NPM particles. The most relevant electroweak precision observables (EWPO) in this context are the W boson mass, M_W , the effective leptonic weak mixing angle, $\sin^2 \theta_{\text{eff}}$, and the anomalous magnetic moment of the muon, $a_\mu \equiv (g-2)_\mu/2$. In models in which a Higgs-boson mass can be predicted, it also constitutes a precision observable, most notably the mass of the lightest \mathcal{CP} -even MSSM Higgs boson, M_h [17]. While the current exclusion bounds on M_h already allow to constrain the MSSM parameter space, the prospective accuracy for the measurement of the mass of a light Higgs boson at the LHC of about 200 MeV [8,9] or at the ILC of even 50 MeV [10–12,18] would promote M_h to a precision observable.

2. Example: The W boson mass

As a prominent example for the interplay of theory and experiment to perform a theory test at the quantum level serves the prediction of the W boson mass, M_W , in the SM and the MSSM. Progress has been achieved over the last decade in the experimental measurements as well as in the theory predictions in the SM and in the MSSM. The current experimental value [14,15,19,20]

$$M_W^{\text{exp}} = 80.398 \pm 25 \text{ GeV} \quad (1)$$

is based on a combination of the LEP results [21,22] and the latest CDF measurement [19,20]. The experimental measurement of M_W also required substantial theory input such as cross section evaluations for LEP [23,24] or kinematics of W and Z boson decays [25] or the inclusion of initial and final state photons [26] at the Tevatron.

Concerning the theory prediction, the W boson mass can be evaluated from

$$M_W^2 \left(1 - \frac{M_W^2}{M_Z^2} \right) = \frac{\pi\alpha}{\sqrt{2}G_F} (1 + \Delta r), \quad (2)$$

where α is the fine structure constant and G_F the Fermi constant. The radiative corrections are summarized in the quantity Δr [27]. Within the SM the one-loop [27] and the complete two-loop result has been obtained for M_W [28–32]. The latter consists of the fermionic electroweak two-loop contributions [28], the purely bosonic two-loop contributions [29] and the QCD corrections of $\mathcal{O}(\alpha\alpha_s)$ [30,31]. Higher-order QCD corrections are known at $\mathcal{O}(\alpha\alpha_s^2)$ [33,34]. Leading electroweak contributions of order $\mathcal{O}(G_F^2\alpha_s m_t^4)$ and $\mathcal{O}(G_F^3 m_t^6)$ that enter via the quantity $\Delta\rho$ [35] have been calculated in Refs. [36–38]. The class of four-loop contributions obtained in Ref. [39] give rise to a numerically negligible effect. The prediction for M_W within the SM (or the MSSM) is obtained by evaluating Δr in these models and solving Eq. (2) for M_W .

Within the MSSM the most precise available result for M_W has been obtained in Ref. [40]. Besides the full SM result, for the MSSM it includes the full

set of one-loop contributions [41,42,40] as well as the corrections of $\mathcal{O}(\alpha_s)$ [43] and of $\mathcal{O}(\alpha_{t,b}^2)$ [44,45] to the quantity $\Delta\rho$; see Ref. [40] for details.

The experimental result and the theory prediction of the SM and the MSSM are compared in Fig. 1.¹ The predictions within the two models give rise to two bands in the m_t – M_W plane with only a relatively small overlap sliver (indicated by a dark-shaded (blue) area in Fig. 1). The allowed parameter region in the SM (the medium-shaded (red) and dark-shaded (blue) bands) arises from varying the only free parameter of the model, the mass of the SM Higgs boson, from $M_H^{\text{SM}} = 114$ GeV, the LEP exclusion bound [46] (upper edge of the dark-shaded (blue) area), to 400 GeV (lower edge of the medium-shaded (red) area). The light shaded (green) and the dark-shaded (blue) areas indicate allowed regions for the unconstrained MSSM, obtained from scattering the relevant parameters independently [40]. The decoupling limit with SUSY masses of $\mathcal{O}(2 \text{ TeV})$ yields the lower edge of the dark-shaded (blue) area. Thus, the overlap region between the predictions of the two models corresponds in the SM to the region where the Higgs boson is light, i.e. in the MSSM allowed region ($M_h \lesssim 135$ GeV [47,48]). In the MSSM it corresponds to the case where all superpartners are heavy, i.e. the decoupling region of the MSSM. The current 68 and 95% C.L. experimental results for m_t [49],

$$m_t^{\text{exp}} = 170.9 \pm 1.8 \text{ GeV}, \quad (3)$$

and M_W are indicated in the plot. As can be seen from Fig. 1, the current experimental 68% C.L. region for m_t and M_W exhibits a slight preference of the MSSM over the SM; only at the 95% C.L. the experimental values enter the SM parameter space. This example indicates that the experimental measurement of M_W in combination with m_t prefers within the SM a relatively small value of M_H^{SM} , or with the MSSM not too heavy SUSY mass scales.

¹The plot shown here is an update of Refs. [41,17,40].

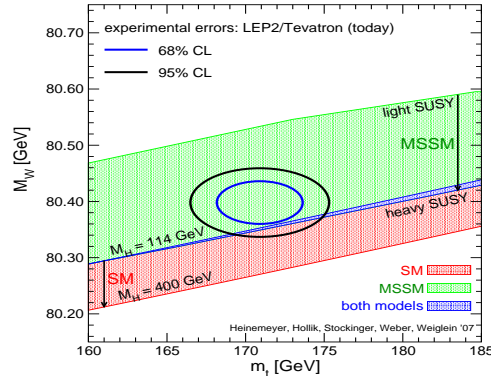


Figure 1. Prediction for M_W in the MSSM and the SM (see text) as a function of m_t in comparison with the present experimental results for M_W and m_t [40].

3. The anomalous magnetic moment of the muon

Another important EWPO which is important in the context of precision tests of the electroweak theory is the anomalous magnetic moment of the muon, $a_\mu \equiv (g - 2)_\mu/2$. For the interpretation of the a_μ results in the context of a NPM the current status of the comparison of the SM prediction with the experimental result is crucial, see Refs. [50–54] for reviews. a_μ is related to the photon–muon vertex function $\Gamma_{\mu\bar{\mu}A^\rho}$ as follows:

$$\begin{aligned} & \bar{u}(p') \Gamma_{\mu\bar{\mu}A^\rho}(p, -p', q) u(p) \\ &= \bar{u}(p') [\gamma_\rho F_V(q^2) \\ & \quad + (p + p')_\rho F_M(q^2) + \dots] u(p), \end{aligned} \quad (4)$$

$$a_\mu = -2m_\mu F_M(0). \quad (5)$$

The SM prediction for the anomalous magnetic moment of the muon depends on the evaluation of QED contributions (see Refs. [55,56] for recent updates), the hadronic vacuum polarization and light-by-light (LBL) contributions. The former have been evaluated in Refs. [54,57,58] and the latter in Refs. [59–61]. The evaluations of the hadronic vacuum polarization contributions using e^+e^- and τ decay data give

somewhat different results. In view of the fact that recent e^+e^- measurements tend to confirm earlier results, whereas the correspondence between previous τ data and preliminary data from BELLE is not so clear, and also in view of the additional uncertainties associated with the isospin transformation from τ decay, nowadays the τ results are usually discarded. This gives an estimate based on e^+e^- data [58]:

$$a_\mu^{\text{theo}} = (11\,659\,180.5 \pm 4.4_{\text{had}} \pm 3.5_{\text{LBL}} \pm 0.2_{\text{QED+EW}}) \times 10^{-10}, \quad (6)$$

where the source of each error is labeled. We note that the new e^+e^- data sets that have recently been published in Refs. [62–64] have been partially included in the updated estimate of $(g-2)_\mu$, see also Ref. [65].

The SM prediction is to be compared with the final result of the Brookhaven $(g-2)_\mu$ experiment E821 [16], namely:

$$a_\mu^{\text{exp}} = (11\,659\,208.0 \pm 6.3) \times 10^{-10}, \quad (7)$$

leading to an estimated discrepancy [58,66]

$$a_\mu^{\text{exp}} - a_\mu^{\text{theo}} = (27.5 \pm 8.4) \times 10^{-10}, \quad (8)$$

equivalent to a $3.3\text{-}\sigma$ effect². While it would be premature to regard this deviation as a firm evidence for new physics, it should be noted that this more than 3σ effect has now firmly been established.

Taking the MSSM as an example to explain the 3.3σ effect, the one-loop (and higher-order corrections) have to be evaluated. The complete one-loop contribution to a_μ can be divided into contributions from diagrams with a smuon-neutralino loop and with a sneutrino-chargino loop, see Fig. 2, leading to

$$\Delta a_\mu^{\text{SUSY,1L}} = \Delta a_\mu^{\tilde{\chi}^\pm \tilde{\nu}_\mu} + \Delta a_\mu^{\tilde{\chi}^0 \tilde{\mu}}. \quad (9)$$

The coupling of an external muon to the SUSY particles is enhanced by $\tan\beta$, which can range from ~ 2 to ~ 60 . This can

²Three other recent evaluations yield slightly different numbers [53,54,57], but similar discrepancies with the SM prediction.

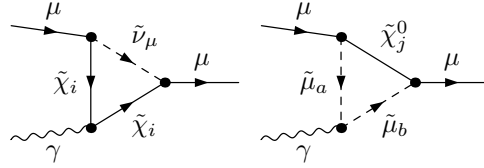


Figure 2. The generic one-loop diagrams for the MSSM contribution to a_μ : diagram with a sneutrino-chargino loop (left) and the diagram with a smuon-neutralino loop (right).

lead to a strong enhancement of the MSSM one-loop diagrams in comparison with the corresponding SM one-loop electroweak diagrams, despite the fact that the masses of the SM particles involved are lighter than the SUSY mass scales. The full one-loop expression can be found in Ref. [67], see Ref. [68] for earlier evaluations. If all SUSY mass scales are set to a common value, $M_{\text{SUSY}} = m_{\tilde{\chi}^\pm} = m_{\tilde{\chi}^0} = m_{\tilde{\mu}} = m_{\tilde{\nu}_\mu}$, the result is given by

$$a_\mu^{\text{SUSY,1L}} = 13 \times 10^{-10} \left(\frac{100 \text{ GeV}}{M_{\text{SUSY}}} \right)^2 \times \tan\beta \text{ sign}(\mu). \quad (10)$$

Obviously, supersymmetric effects can easily account for a $(20 \dots 40) \times 10^{-10}$ deviation, if μ is positive and M_{SUSY} lies roughly between 100 GeV (for small $\tan\beta$) and 600 GeV (for large $\tan\beta$). On the other hand, demanding that SUSY fulfills Eq. (8) at the two or three σ level, Eq. (10) shows that the $(g-2)_\mu$ measurement places strong bounds on the supersymmetric parameter space.

In addition to the full one-loop contributions, the leading QED two-loop corrections have also been evaluated [69]. Further corrections at the two-loop level have been obtained [70,71], leading to corrections to the one-loop result that are $\lesssim 10\%$. These corrections are taken into account in the examples shown below.

Concerning other NPM, the generic size of the new contribution to a_μ is roughly

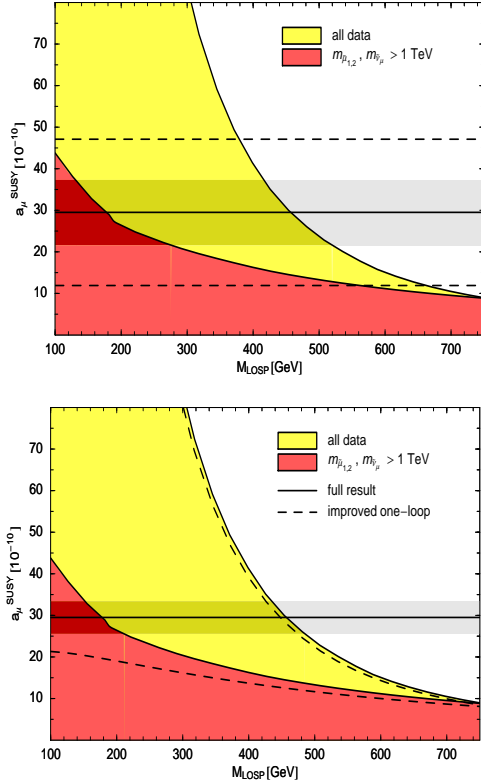


Figure 3. Scan over the MSSM parameter space for a_μ^{SUSY} , including all available one- and two-loop contributions, as a function of the lightest observable particle (the lightest $\tilde{\mu}$ or $\tilde{\chi}_2^0$ or $\tilde{\chi}_1^\pm$) [52]. The light (yellow) shaded region is all data, the dark (red) shaded region has all second generation sleptons heavier than 1 TeV. The upper plot shows the current experimental deviation at the one (shaded strip) or two (dashed lines) σ level. The lower plot shows the full result for a_μ^{SUSY} (full area) and the one-loop result only (dashed lines). Here the shaded strip corresponds to an anticipated future accuracy of 4×10^{-10} (see text).

given in terms of the NPM mass scale M_{NPM} [52],

$$a_\mu^{\text{NPM}} \sim 1 \times 10^{-10} \left(\frac{300 \text{ GeV}}{M_{\text{NPM}}} \right)^2. \quad (11)$$

Thus, the generic NPM contribution is usually too small to explain the 3.3σ effect in Eq. (8). The advantages of SUSY are the $\tan\beta$ enhancement of the muon coupling to SUSY particles and the fact that relatively light SUSY particles with masses $\gtrsim 100$ GeV are experimentally allowed.

In Fig. 3 we show the results of an MSSM parameter scan for a_μ , including all available one- and two-loop contributions, as a function of the lightest observable particle (the lightest $\tilde{\mu}$ or $\tilde{\chi}_2^0$ or $\tilde{\chi}_1^\pm$) [52]. The light (yellow) shaded region is all data, the dark (red) shaded region has all second generation sleptons heavier than 1 TeV. In the lower plot of Fig. 3 the prediction of the one-loop result only is indicated by the dashed lines. It can be clearly seen that making the smuons and charginos/neutralinos heavy suppresses the one-loop diagrams shown in Fig. 2. In this case the two-loop contribution become important [70,71]. The upper plot shows the current one (shaded strip) or two (dashed lines) σ results according to Eq. (8). It can be clearly seen that demanding agreement of the MSSM contribution with the current experimental result imposes strong restrictions on the parameter space.

A new $(g-2)_\mu$ experiment has been proposed, see Ref. [72] and references therein. Together with further improvement on the theory side, the error of $a_\mu^{\text{exp}} - a_\mu^{\text{theo}}$ could be decreased to the level of 4×10^{-10} [52, 72]. The effect of this anticipated future precision can be seen in the lower plot of Fig. 3, assuming the current central deviation. The restrictions on the MSSM parameter space would become very strong. The case with heavy smuons and charginos/neutralinos could only be realized using the SUSY prediction at the two-loop level [70,71].

4. Electric Dipole Moments

A different way for probing NPM is via their contribution to EDMs of heavy quarks, of the electron and the neutron or neutral atoms. Some present limits are

summarized in Tab. 1, see Ref. [73] for a review. Improvements of the sensitivities of $\mathcal{O}(10^1 - 10^2)$ can be expected from ongoing and future experiments, see Ref. [77] (and references therein).

| System | limit | group |
|-------------------|----------------------------------|---------|
| e^- | 1.6×10^{-27} (90% C.L.) | Berkely |
| n | 2.9×10^{-26} (90% C.L.) | ILL |
| ^{199}Au | 2.1×10^{-28} (95% C.L.) | Seattle |

Table 1. Present bounds for EDMs [74–76].

While SM contributions start only at the three-loop level [78], due new complex parameters NPM can contribute already at one-loop order [79]. Taking the MSSM with complex parameters (cMSSM) as a specific example, the respective calculations can be found for heavy quarks in Ref. [80], for the electron and the neutron in Refs. [81,82] and references therein. Recent reviews concerning the EDMs in the cMSSM are given in Refs. [81,83,84].

A generic SUSY diagram is given in Fig. 4 yielding a contribution to the EDM of the neutron, d_n , as [85]

$$\frac{d_n}{m_d} \sim \frac{1}{16\pi^2} \frac{\mu m_{\tilde{g}}}{M_{\text{SUSY}}} \sin \theta_\mu, \quad (12)$$

where m_d is the mass of the down quark, $m_{\tilde{g}}$ denotes the gluino mass, and μ is the Higgs mixing parameter with its phase θ_μ . Also the leading two-loop corrections for the electron and neutron EDMs are available [82,86]. Large phases in the first two generations of (s)fermions can only be accommodated if these generations are assumed to be very heavy [87] or large cancellations occur [88], see however the discussion in Ref. [83]. EDMs thus place already strong bounds on the size of the complex phases of the cMSSM (see e.g. Ref. [89]) and have to be taken into account in any related phenomenological analysis.

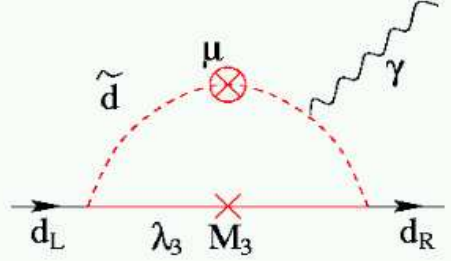


Figure 4. Generic SUSY diagram contributing to the EDM of the neutron.

5. EWPO in the SM

Within the SM the EWPO have been used to constrain the last unknown parameter of the model, the Higgs-boson mass M_H^{SM} . Originally the EWPO comprise over thousand measurements of “realistic observables” (with partially correlated uncertainties) such as cross sections, asymmetries, branching ratios etc. This huge set is reduced to 17 so-called “pseudo observables” by the LEP [14] and Tevatron [15] Electroweak working groups. The “pseudo observables” (again called EWPO in the following) comprise the W boson mass M_W (see Sect. 2), the width of the W boson, Γ_W , as well as various Z pole observables: the effective weak mixing angle, $\sin^2 \theta_{\text{eff}}$, Z decay widths to SM fermions, $\Gamma(Z \rightarrow f\bar{f})$, the invisible and total width, Γ_{inv} and Γ_Z , forward-backward and left-right asymmetries, A_{FB}^f and A_{LR}^f , and the total hadronic cross section, σ_{had}^0 . The Z pole results including their combination are final [22]. Experimental progress from the Tevatron comes for M_W and m_t . (Also the error combination for M_W and Γ_W from the four LEP experiments has not been finalized yet due to not-yet-final analyses on the color-reconnection effects.)

The EWPO that give the strongest constraints on M_H^{SM} are M_W , A_{FB}^b and A_{LR}^e . The value of $\sin^2 \theta_{\text{eff}}$ is extracted from a combination of various A_{FB}^f and A_{LR}^f , where A_{FB}^b and A_{LR}^e give the dominant con-

tribution.

The one-loop contributions to Δr (i.e. to M_W , see Eq. (2)) can be decomposed as follows [27],

$$\Delta r_{1\text{-loop}} = \Delta\alpha - \frac{c_w^2}{s_w^2} \Delta\rho + \Delta r_{\text{rem}}(M_H^{\text{SM}}). \quad (13)$$

The first term, $\Delta\alpha$ contains large logarithmic contributions as $\log(M_Z/m_f)$ and amounts $\sim 6\%$. The second term contains the ρ parameter [35], being $\Delta\rho \sim m_t^2$ (with $c_w^2 = M_W^2/M_Z^2$, $s_w^2 = 1 - c_w^2$). This term amounts $\sim 3.3\%$. The final term in Eq. (13) is $\Delta r_{\text{rem}} \sim \log(M_H^{\text{SM}}/M_W)$, and with a size of $\sim 1\%$ correction yields the constraints on M_H^{SM} . The fact that the leading correction involving M_H^{SM} is logarithmic also applies to the other EWPO. Starting from two-loop order, also terms $\sim (M_H^{\text{SM}}/M_W)^2$ appear. The SM prediction of M_W as a function of m_t for the range $M_H^{\text{SM}} = 114 \text{ GeV} \dots 1000 \text{ GeV}$ is shown as the dark shaded (green) band in Fig. 5 [14]. The upper edge with $M_H^{\text{SM}} = 114 \text{ GeV}$ corresponds to the lower limit on M_H^{SM} obtained at LEP [46]. The prediction is compared with the direct experimental result (dotted/blue ellipse) and with the indirect results for M_W and m_t as obtained from EWPO (solid/red ellipse). Consistent with Fig. 1 the direct experimental result at the 68% C.L. does not enter the SM prediction, i.e. low SM Higgs boson masses, $M_H^{\text{SM}} \sim 44 \text{ GeV}$ [90], are preferred by the measurement of M_W and m_t .

The effective weak mixing angle is evaluated from various asymmetries and other EWPO as shown in Fig. 6 [20]. The average determination yields $\sin^2 \theta_{\text{eff}} = 0.23153 \pm 0.00016$ with a $\chi^2/\text{d.o.f}$ of 11.8/5, corresponding to a probability of 3.7% [20]. The large χ^2 is driven by the two single most precise measurements, A_{LR}^e by SLD and A_{FB}^b by LEP, where the earlier (latter) one prefers a value of $M_H^{\text{SM}} \sim 32(437) \text{ GeV}$ [90]. The two measurements differ by more than 3σ . The averaged value of $\sin^2 \theta_{\text{eff}}$, as shown in Fig. 6, prefers $M_H^{\text{SM}} \sim 110 \text{ GeV}$ [90].

The indirect M_H^{SM} determination for sev-

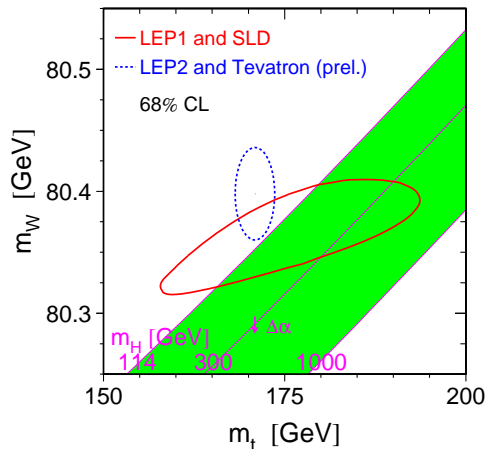


Figure 5. Prediction for M_W in the SM as a function of m_t for the range $M_H^{\text{SM}} = 114 \text{ GeV} \dots 1000 \text{ GeV}$ [14]. The prediction is compared with the present experimental results for M_W and m_t as well as with the indirect constraints obtained from EWPO.

eral individual EWPO is given in Fig. 7. Shown are the central values of M_H^{SM} and the one σ errors [14]. The dark shaded (green) vertical band indicates the combination of the various single measurements in the 1σ range. The vertical line shows the lower LEP bound for M_H^{SM} [46]. It can be seen that M_W , A_{LR}^e and A_{FB}^b give the most precise indirect M_H^{SM} determination, where only the latter one pulls the preferred M_H^{SM} value up, yielding an averaged value of [14]

$$M_H^{\text{SM}} = 76_{26}^{+33} \text{ GeV} , \quad (14)$$

still compatible with the direct LEP bound of [46]

$$M_H^{\text{SM}} \geq 114.4 \text{ GeV at } 95\% \text{ C.L.} \quad (15)$$

Thus, the measurement of A_{FB}^b prevents the SM from being incompatible with the direct bound and the indirect constraints on M_H^{SM} .

Finally, in Fig. 8 [14] we show the result for the global fit to M_H^{SM} including all EWPO. $\Delta\chi^2$ is shown as a function

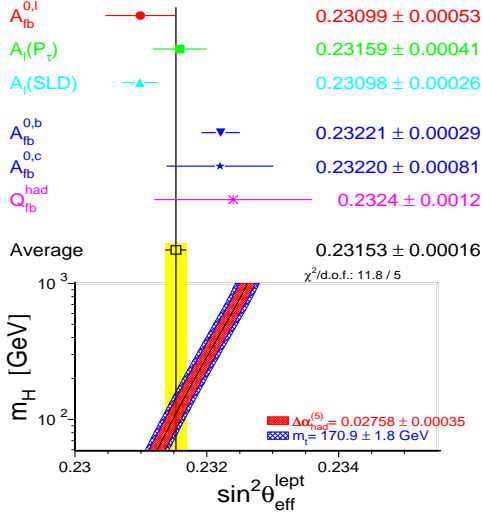


Figure 6. Prediction for $\sin^2 \theta_{\text{eff}}$ in the SM as a function of M_H^{SM} for $m_t = 170.9 \pm 1.8 \text{ GeV}$ and $\Delta\alpha_{\text{had}}^{(5)} = 0.02758 \pm 0.00035$ [20]. The prediction is compared with the present experimental results for $\sin^2 \theta_{\text{eff}}$ as averaged over several individual measurements.

of M_H^{SM} , yielding Eq. (14) as best fit with an upper limit of 144 GeV at 95% C.L. This value increases to 182 GeV if the direct LEP bound of Eq. (15) is included in the fit. The theory (intrinsic) uncertainty in the SM calculations (as evaluated with TOPAZ0 [91] and ZFITTER [92]) are represented by the thickness of the blue band. The width of the parabola itself, on the other hand, is determined by the experimental precision of the measurements of the EWPO and the input parameters.

The current and anticipated future experimental uncertainties for $\sin^2 \theta_{\text{eff}}$, M_W and m_t are summarized in Tab. 2. Also shown is the relative precision of the indirect determination of M_H^{SM} [20]. Each column represents the combined results of all detectors and channels at a given collider, taking into account correlated systematic uncertainties, see Refs. [93–96] for details. The indirect M_H^{SM} determination has to be

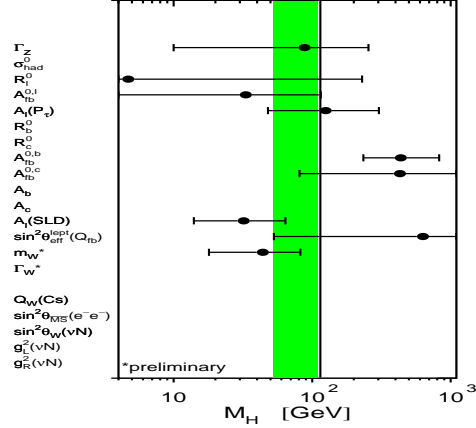


Figure 7. Indirect constraints on M_H^{SM} from various EWPO. Shown are the central values and the one σ errors [14]. The dark shaded (green) vertical band indicates the combination of the various single measurements in the 1σ range. The vertical line shows the lower bound of $M_H^{\text{SM}} \geq 114.4 \text{ GeV}$ obtained at LEP [46].

compared with the (possible) direct measurement at the LHC [8,9] and the ILC [10–12,18],

$$\delta M_H^{\text{SM,exp,LHC}} \approx 200 \text{ MeV}, \quad (16)$$

$$\delta M_H^{\text{SM,exp,ILC}} \approx 50 \text{ MeV}. \quad (17)$$

This comparison will shed light on the basic theoretical components for generating the masses of the fundamental particles. On the other hand, an observed inconsistency would be a clear indication for the existence of a new physics scale.

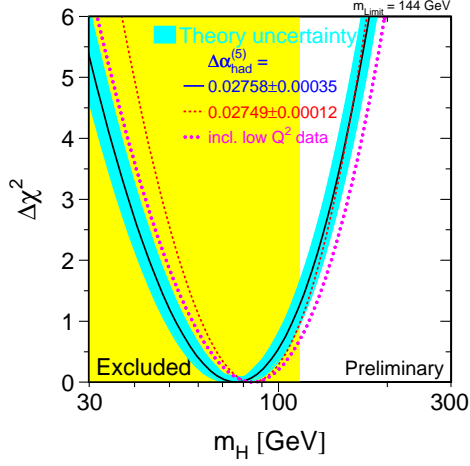


Figure 8. $\Delta\chi^2$ curve derived from all EWPO measured at LEP, SLD, CDF and D0, as a function of M_H^{SM} , assuming the SM to be the correct theory of nature [14].

6. EWPO in the MSSM

As compared to the SM there are new additional contributions to EWPO in the MSSM that can be sizable:

1. While in the SM the leading corrections to e.g. the ρ parameter (i.e. to gauge boson self-energies) arise from t/b loops, in the MSSM large corrections can arise from \tilde{t}/\tilde{b} loops ($V = Z, W^\pm$):
-
2. New \mathcal{CP} -violating effects can arise from new complex parameters, see Sect. 4.
 3. Yukawa corrections $\sim m_t^4 \log\left(\frac{m_{\tilde{t}_1} m_{\tilde{t}_2}}{m_t^2}\right)$ can give large contributions.
 4. Corrections from the b/\tilde{b} sector are enhanced by $\tan\beta$ and can become sizable, see also Sect. 3.

| | now | Tevatron | LHC |
|---|-----|----------------|-------|
| $\delta \sin^2 \theta_{\text{eff}} (\times 10^5)$ | 16 | — | 14–20 |
| δM_W [MeV] | 25 | 20 | 15 |
| δm_t [GeV] | 1.8 | 1.2 | 1.0 |
| $\delta M_H^{\text{SM}}/M_H^{\text{SM}}$ [%] | 37 | | 28 |
| | ILC | ILC with GigaZ | |
| $\delta \sin^2 \theta_{\text{eff}} (\times 10^5)$ | — | 1.3 | |
| δM_W [MeV] | 10 | 7 | |
| δm_t [GeV] | 0.2 | 0.1 | |
| $\delta M_H^{\text{SM}}/M_H^{\text{SM}}$ [%] | | 16 | |

Table 2

Current and anticipated future experimental uncertainties for $\sin^2 \theta_{\text{eff}}$, M_W and m_t . Also shown is the relative precision of the indirect determination of M_H^{SM} [20]. Each column represents the combined results of all detectors and channels at a given collider, taking into account correlated systematic uncertainties, see Refs. [93–96] for details.

5. In general SUSY corrections are relevant if the new mass scales are (relatively) small. On the other hand, non-decoupling SUSY effects $\sim \log \frac{M_{\text{SUSY}}}{M_W}$ can become important for large values of M_{SUSY} .

The example of the W boson mass has been discussed in Sect. 2. In the same spirit also the $\sin^2 \theta_{\text{eff}}$ has been evaluated in the MSSM and compared to the SM prediction [97]. A parameter scan similar to the one shown in Fig. 1 reveals no preference for either model. This result, as the not too low best-fit value for M_H^{SM} is largely driven by the measurement of A_{FB}^b , while A_{LR}^e has a clear preference for the MSSM prediction.

Another EWPO in the MSSM is the mass of the lightest Higgs boson, M_h . In the MSSM two Higgs doublets are required, resulting in five physical Higgs bosons: the light and heavy \mathcal{CP} -even h and H , the \mathcal{CP} -

odd A , and the charged Higgs bosons H^\pm . The Higgs sector of the MSSM can be expressed at lowest order in terms of M_Z , M_A and $\tan\beta$. All other masses and mixing angles can therefore be predicted. At the tree-level this leads to the prediction of $M_h^{\text{tree}} \leq M_Z$. However, the tree-level bound on M_h , being obtained from the gauge couplings, receives large corrections from SUSY-breaking effects in the Yukawa sector of the theory. The leading one-loop correction is proportional to m_t^4 . The leading logarithmic one-loop term (for vanishing mixing between the scalar top quarks) reads [98]

$$\Delta M_h^2 = \frac{3G_F m_t^4}{\sqrt{2}\pi^2 \sin^2\beta} \log\left(\frac{m_{\tilde{t}_1} m_{\tilde{t}_2}}{m_t^2}\right). \quad (18)$$

Corrections of this kind have drastic effects on the predicted value of M_h and many other observables in the MSSM Higgs sector. The one-loop corrections can shift M_h by 50–100%. In this way the MSSM Higgs sector, and especially M_h , depend sensitively on the other MSSM parameters; M_h will be the most powerful precision observable in the MSSM.

The status of higher-order corrections to the masses (and the mixing) in the Higgs sector of the MSSM³ is quite advanced. The complete one-loop result within the MSSM is known [98,101–103]. The by far dominant one-loop contribution is the $\mathcal{O}(\alpha_t)$ term due to top and stop loops ($\alpha_t \equiv h_t^2/(4\pi)$, h_t being the top-quark Yukawa coupling). The computation of the two-loop corrections has meanwhile reached a stage where all the presumably dominant contributions are available [47,104–110], see Refs. [48,17] for reviews. In particular, the $\mathcal{O}(\alpha_t\alpha_s)$, $\mathcal{O}(\alpha_t^2)$, $\mathcal{O}(\alpha_b\alpha_s)$, $\mathcal{O}(\alpha_t\alpha_b)$ and $\mathcal{O}(\alpha_b^2)$ contributions to the self-energies are known for vanishing external momenta. For the (s)bottom corrections, which are mainly relevant for large values of $\tan\beta$, an all-order resummation of the $\tan\beta$ -enhanced term of $\mathcal{O}(\alpha_b(\alpha_s \tan\beta)^n)$ is performed [111,

112]. The remaining theoretical uncertainty on the lightest \mathcal{CP} -even Higgs boson mass has been estimated to be below ~ 3 GeV [48,17,113]. The above calculations have been implemented into public codes. The program **FeynHiggs** [47,48,99, 114] is based on the results obtained in the Feynman-diagrammatic (FD) approach and includes all the above corrections. The code **CPsuperH** [115] is based on the renormalization group (RG) improved effective potential approach. Most recently a full two-loop effective potential calculation (including even the momentum dependence for the leading pieces and the leading three-loop corrections) has been published [116]. However, no computer code is publicly available.

While a precise knowledge of m_t is important for M_W , $\sin^2\theta_{\text{eff}}$, \dots , it is *crucial* for M_h , see also Ref. [117]. Due to the strong dependence of M_h on m_t , see Eq. (18), by numerical coincidence

$$\delta m_t^{\text{exp}}/\delta M_h^{\text{theo}} \approx 1 \quad (19)$$

holds [118]. Thus already the LHC precision for M_h , Eq. (16), requires the ILC precision for m_t , see Tab. 2. (More examples of such LHC/ILC interplay can be found in Ref. [13].)

7. EWPO in the CMSSM

In order to achieve a simplification of the plethora of soft SUSY-breaking parameters appearing in the general MSSM, one assumption that is frequently employed is that (at least some of) the soft SUSY-breaking parameters are universal at some high input scale, before renormalization. One model based on this simplification is the constrained MSSM (CMSSM), in which all the soft SUSY-breaking scalar masses m_0 are assumed to be universal at the GUT scale, as are the soft SUSY-breaking gaugino masses $m_{1/2}$ and trilinear couplings A_0 . Further parameters are $\tan\beta$ and the sign of the Higgs mixing parameter μ . Since the low-scale parameters in this scenario are derived from a small set of input quantities, it is meaningful to combine various exper-

³We concentrate here on the case with real parameters. For complex parameters see Refs. [99,100] and references therein.

imental constraints. The EWPO can be supplemented with B physics observables (BPO) and astrophysical results such as the cold dark matter (CDM) abundance.

As an example we show the prediction for M_W in the CMSSM [119]. The parameter points are chosen such that they yield the correct value of the CDM density inferred from WMAP and other data, namely [120]

$$0.094 < \Omega_{\text{CDM}} h^2 < 0.129. \quad (20)$$

The fact that the density is relatively well known restricts the SUSY parameter space to a thin, fuzzy ‘WMAP hypersurface’ [121, 122], effectively reducing its dimensionality by one. The analysis has been performed on ‘WMAP lines’ in the $(m_{1/2}, m_0)$ planes for discrete values of the other SUSY parameters: $\tan \beta = 10, 50$ and $A_0 = 0, \pm 1, \pm 2 \times m_{1/2}$. In Fig. 9 the CMSSM prediction for M_W is shown as a function of $m_{1/2}$. The center (solid) line is the present central experimental value, and the (solid) outer lines show the current $\pm 1\text{-}\sigma$ range. The dashed lines correspond to the full error including also parametric and intrinsic uncertainties. One can see in that the variation with A_0 is relatively weak for both values of $\tan \beta$. The best results are obtained for low $m_{1/2}$, while large values lead to a $\sim 1.5\sigma$ deviation (corresponding to the SM limit).

In Ref. [119] five EWPO (M_W , $\sin^2 \theta_{\text{eff}}$, Γ_Z , $(g-2)_\mu$ and M_h) and four BPO ($\text{BR}(b \rightarrow s\gamma)$, $\text{BR}(B_s \rightarrow \mu^+ \mu^-)$, $\text{BR}(B_u \rightarrow \tau \nu_\tau)$ and ΔM_{B_s}) are used to perform a χ^2 analysis. For M_h and $\text{BR}(B_s \rightarrow \mu^+ \mu^-)$ no experimental observation but the full experimental exclusion bounds (as translated into χ^2) have been used. Within the CMSSM the lightest Higgs boson has SM-like production and decay properties [123, 124], and the SM results [46] can be used. The other parameters are $m_t = 171.4 \pm 2.1$ GeV and $m_b(m_b) = 4.25 \pm 0.11$ GeV, and m_0 is chosen to yield the central value of the cold dark matter density indicated by WMAP and other observations for the central values of m_t and $m_b(m_b)$. The total χ^2 as a function of $m_{1/2}$ is shown in Fig. 10. One can see a global minimum of $\chi^2 \sim 4.5$ for

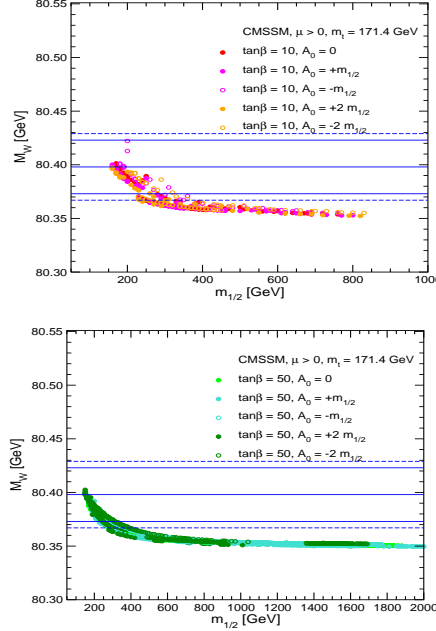


Figure 9. The CMSSM predictions for M_W are shown as functions of $m_{1/2}$ along the WMAP strips for $\tan \beta = 10$ (upper) and $\tan \beta = 50$ (lower plot) for various A_0 values [119]. In each panel, the center (solid) line is the present central experimental value, and the (solid) outer lines show the current $\pm 1\text{-}\sigma$ range. The dashed lines correspond to the full error including also parametric and intrinsic uncertainties.

both values of $\tan \beta$. This is quite a good fit for the number of experimental observables being fitted. Such a preference for not too heavy SUSY particles has also been found in several other analyses [125–128], see also Refs. [129, 130].

The $m_{1/2}$ - χ^2 relation can be translated into a prediction of SUSY masses. As an example Fig. 11 shows the mass of the lighter $\tilde{\tau}$ together with the corresponding χ^2 value [119]. For $\tan \beta = 10(50)$ the preferred value is $\tilde{\tau}_1 \approx 150(250)$ GeV. In this way the EWPO analysis offers good prospects for the LHC and the ILC and possibly even for the Tevatron. In a sim-

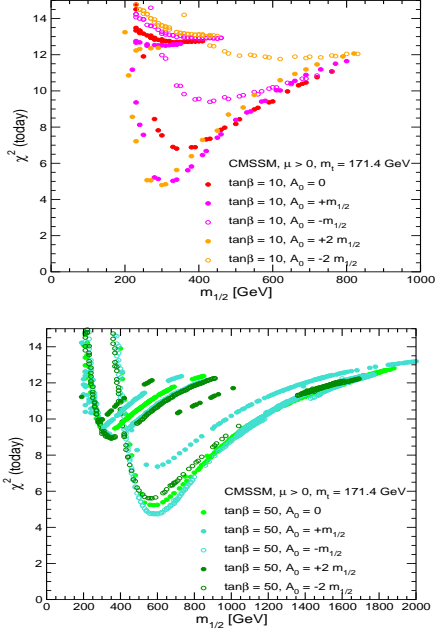


Figure 10. The combined χ^2 function for the EWPO M_W , $\sin^2 \theta_{\text{eff}}$, Γ_Z , $(g-2)_\mu$, M_h , and the BPO $\text{BR}(b \rightarrow s\gamma)$, $\text{BR}(B_s \rightarrow \mu^+ \mu^-)$, $\text{BR}(B_u \rightarrow \tau \nu_\tau)$ and ΔM_{B_s} , evaluated in the CMSSM for $\tan \beta = 10$ (upper) and $\tan \beta = 50$ (lower plot) for various discrete values of A_0 [119].

ilar way also M_h with its corresponding χ^2 can be analyzed. The LEP limit of 114.4 GeV as a lower bound and the upper bound of $M_h^{\text{CMSSM}} \lesssim 127$ GeV [17,131] naturally squeeze the M_h prediction into this interval. More interesting is the case where the lower LEP bound is left out. In this case, using four EWPO, four BPO and the CDM constraint a best-fit value for M_h of $\sim 110 \dots 115$ GeV (depending on $\tan \beta$) was obtained [119]. This is substantially higher than the SM result of Eq. (14).

A fit as close as possible to the SM fit for M_H^{SM} (resulting in Fig. 8) has been performed in Ref. [128]. All EWPO as in the SM [14] (except Γ_W , which has a minor impact) were included, supplemented by the CDM constraint in Eq. (20), the $(g-2)_\mu$

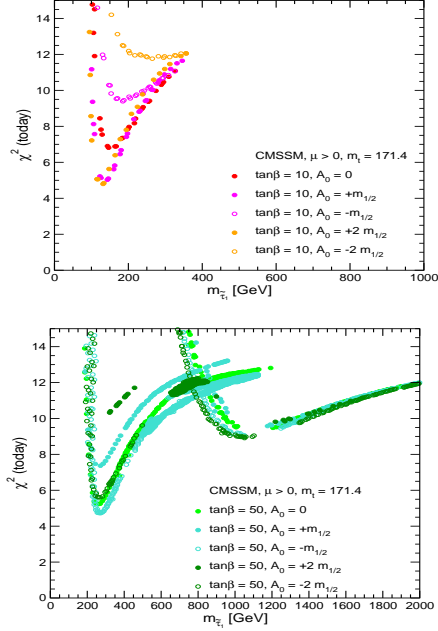


Figure 11. The mass of the lighter $\tilde{\tau}$ with its χ^2 values [119].

results in Eq. (8) and the $\text{BR}(b \rightarrow s\gamma)$ constraint. The χ^2 is minimized with respect to all CMSSM parameters for each point of this scan. Therefore, $\Delta\chi^2 = 1$ represents the 68% confidence level uncertainty on M_h . Since the direct Higgs boson search limit from LEP is not used in this scan the lower bound on M_h arises as a consequence of *indirect* constraints only, as in the SM fit.

In the left plot of Fig. 12 [128] the $\Delta\chi^2$ is shown as a function of M_h in the CMSSM. The area with $M_h \geq 127$ is theoretically inaccessible, see above. The right plot of Fig. 12 shows the red band parabola from the CMSSM in comparison with the blue band parabola from the SM. There is a well defined minimum in the red band parabola, leading to a prediction of [128]

$$M_h^{\text{CMSSM}} = 110_{-10}^{+8} (\text{exp}) \pm 3 (\text{th}) \text{ GeV}, (21)$$

where the first, asymmetric uncertainties are experimental and the second uncertainty is theoretical (from the unknown higher-order corrections to M_h [48,17]).

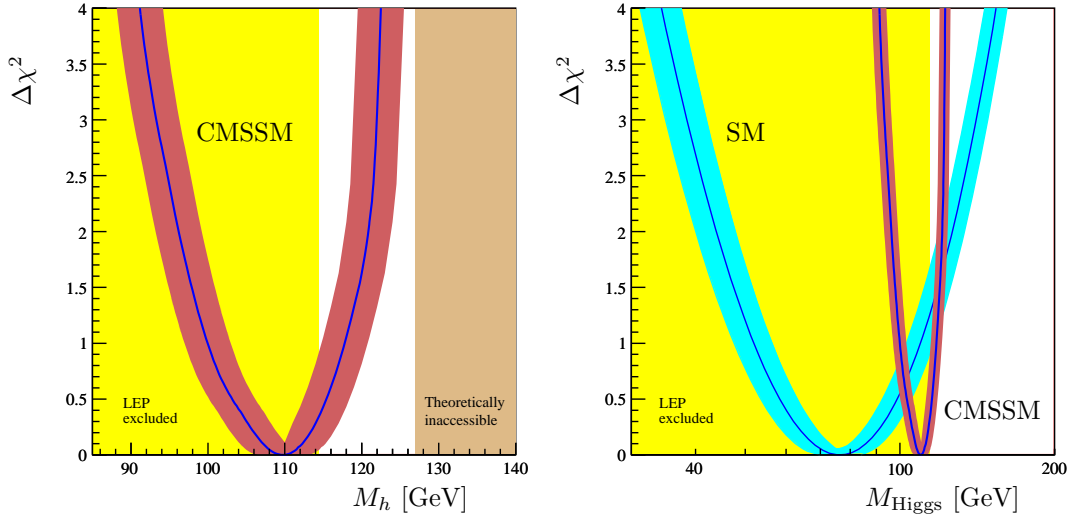


Figure 12. Left: Scan of the lightest Higgs boson mass versus $\Delta\chi^2$. The curve is the result of a CMSSM fit using all of the available constraints (see text). The direct limit on M_h from LEP [46,132] is not included. The red (dark gray) band represents the total theoretical uncertainty from unknown higher-order corrections, and the dark shaded area on the right above 127 GeV is theoretically inaccessible (see text). Right: Scan of the Higgs boson mass versus $\Delta\chi^2$ for the SM (blue/light gray), as determined by [14] using all available electroweak constraints, and for comparison, with the CMSSM scan superimposed (red/dark gray).

The fact that the minimum in Fig. 12 is sharply defined is a general consequence of the MSSM, where the neutral Higgs boson mass is not a free parameter as described above. The theoretical upper bound $M_h \lesssim 135(127)$ GeV in the (C)MSSM explains the sharper rise of the $\Delta\chi^2$ at large M_h values and the asymmetric uncertainty. In the SM, M_H^{SM} is a free parameter and only enters (at leading order) logarithmically in the prediction of the precision observables. In the (C)MSSM this logarithmic dependence is still present, but in addition M_h depends on m_t and the SUSY parameters, mainly from the scalar top sector. The low-energy SUSY parameters in turn are all connected via RGEs to the GUT scale parameters. The sensitivity on M_h in the analysis of Ref. [128] (and also of Ref. [119]) is therefore the combination of the indirect constraints on the four free CMSSM parameters and the fact that M_h is directly predicted in terms of these parameters. This sensitivity also gives rise to the fact that the fit result in the CMSSM is less affected by the uncertainties from unknown higher-order corrections in the predictions of the electroweak precision observables.

While the theoretical uncertainty of the CMSSM fit (red/dark gray band in Fig. 12) is dominated by the higher-order uncertainties in the prediction for M_h , the theoretical uncertainty of the SM fit (blue/light gray band in Fig. 12) is dominated by the higher-order uncertainties in the prediction for the effective weak mixing angle, $\sin^2\theta_{\text{eff}}$ [133]. The most striking feature is that even *without* the direct experimental lower limit from LEP of 114.4 GeV the CMSSM prefers a Higgs boson mass which is quite close to and compatible with this bound. From the curve in Fig. 12, the value of the χ^2 at the LEP limit corresponds to a probability of 20% (including theoretical errors in the red band). This probability may be compared with the SM with a 12% χ^2 probability at the LEP limit (including theoretical errors from the blue band).

Acknowledgements

We thank the organizers of *Lepton Photon 07* for the invitation and financial support. We furthermore thank A. Ritz, D. Stöckinger and G. Weiglein for help in the preparation of this talk and M. Grünewald for helpful discussions.

REFERENCES

1. S. Glashow, *Nucl. Phys.* **22** (1961) 579; S. Weinberg, *Phys. Rev. Lett.* **19** (1967) 19; A. Salam, in: *Proceedings of the 8th Nobel Symposium*, Editor N. Svartholm, Stockholm, 1968.
2. H. Nilles, *Phys. Rept.* **110** (1984) 1; H. Haber and G. Kane, *Phys. Rept.* **117** (1985) 75; R. Barbieri, *Riv. Nuovo Cim.* **11** (1988) 1.
3. J. Gunion, H. Haber, G. Kane and S. Dawson, *The Higgs Hunter's Guide* (Perseus Publishing, Cambridge, MA, 1990), and references therein.
4. N. Arkani-Hamed, A. Cohen and H. Georgi, *Phys. Lett. B* **513** (2001) 232 [arXiv:hep-ph/0105239]; N. Arkani-Hamed, A. Cohen, T. Gregoire and J. Wacker, *JHEP* **0208** (2002) 020 [arXiv:hep-ph/0202089]; for a review see: M. Schmaltz and D. Tucker-Smith, *Ann. Rev. Nucl. Part. Sci.* **55** (2005) 229 [arXiv:hep-ph/0502182].
5. N. Arkani-Hamed, S. Dimopoulos and G. Dvali, *Phys. Lett. B* **429** (1998) 263 [arXiv:hep-ph/9803315]; *Phys. Lett. B* **436** (1998) 257 [arXiv:hep-ph/9804398]; I. Antoniadis, *Phys. Lett. B* **246** (1990) 377; J. Lykken, *Phys. Rev. D* **54** (1996) 3693 [arXiv:hep-th/9603133]; I. Antoniadis and M. Quiros, *Phys. Lett. B* **392** (1997) 61 [arXiv:hep-th/9609209]; L. Randall and R. Sundrum, *Phys. Rev. Lett.* **83** (1999) 3370 [arXiv:hep-ph/9905221]; for reviews see: J. Hewett and M. Spiropulu, *Ann. Rev. Nucl. Part. Sci.* **52** (2002) 397 [arXiv:hep-ph/0205106]; T. Rizzo, arXiv:hep-ph/0409309; C. Csaki, J. Hubisz and P. Meade, arXiv:hep-ph/0510275.
6. W. Yao et al. [Particle Data Group Collaboration], *J. Phys. G* **33** (2006) 1.
7. See: www-cdf.fnal.gov/physics/projections/.
8. ATLAS Collaboration, *Detector and Physics Performance Technical Design Report*, CERN/LHCC/99-15 (1999), see: atlasinfo.cern.ch/Atlas/GROUPS/PHYSICS/TDR/access.html.
9. CMS Collaboration, *CMS Physics Technical Design Report, Volume 2. CERN/LHCC 2006-021*, see: cmsdoc.cern.ch/cms/cpt/tdr/.
10. J. Aguilar-Saavedra et al., TESLA TDR Part 3: "Physics at an e^+e^- Linear Collider" [arXiv:hep-ph/0106315], see: tesla.desy.de/tdr/; K. Ackermann et al., DESY-PROC-2004-01.
11. T. Abe et al. [American Linear Collider Working Group Collaboration], *Resource book for Snowmass 2001*, arXiv:hep-ex/0106055; arXiv:hep-ex/0106056; arXiv:hep-ex/0106057.
12. K. Abe et al. [ACFA Linear Collider Working Group Collaboration], arXiv:hep-ph/0109166.
13. G. Weiglein et al. [LHC/ILC Study Group], *Phys. Rept.* **426** (2006) 47 [arXiv:hep-ph/0410364].
14. LEP Electroweak Working Group, see: lepewwg.web.cern.ch/LEPEWWG/Welcome.html.
15. Tevatron Electroweak Working Group, see: tevewwg.fnal.gov.
16. G. Bennett et al. [The Muon g-2 Collaboration], *Phys. Rev. D* **73** (2006) 072003 [arXiv:hep-ex/0602035].
17. S. Heinemeyer, W. Hollik and G. Weiglein, *Phys. Rept.* **425** (2006) 265 [arXiv:hep-ph/0412214].
18. S. Heinemeyer et al., arXiv:hep-ph/0511332.
19. T. Aaltonen et al. [CDF Collaboration], arXiv:0707.0085 [hep-ex].
20. M. Grünewald, arXiv:0709.3744 [hep-ex]; arXiv:0710.2838 [hep-ex].
21. M. Grünewald et al., arXiv:hep-ph/0005309.
22. The ALEPH, DELPHI, L3, OPAL, SLD Collaborations, the LEP Electroweak Working Group, the SLD Electroweak and Heavy Flavour Groups, *Phys. Rept.* **427** (2006) 257 [arXiv:hep-ex/0509008]; [The ALEPH, DELPHI, L3 and OPAL Collaborations, the LEP Electroweak Working Group],

- arXiv:hep-ex/0612034.
23. A. Denner, S. Dittmaier, M. Roth and D. Wackeroth, *Nucl. Phys.* **560** (1999) 33 [arXiv:hep-ph/9904472]; *Nucl. Phys. B* **587** (2000) 67 [arXiv:hep-ph/0006307]; *Comput. Phys. Commun.* **153** (2003) 462 [arXiv:hep-ph/0209330].
 24. S. Jadach, W. Placzek, M. Skrzypek, B. Ward and Z. Was, *Phys. Rev. D* **65** (2002) 093010 [arXiv:hep-ph/0007012]; *Comput. Phys. Commun.* **140** (2001) 432 [arXiv:hep-ph/0103163].
 25. C. Balazs and C. P. Yuan, *Phys. Rev.* **56** (1997) 5558 [arXiv:hep-ph/9704258].
 26. U. Baur, S. Keller and D. Wackeroth, *Phys. Rev. D* **59** (1999) 013002 [arXiv:hep-ph/9807417].
 27. A. Sirlin, *Phys. Rev. D* **22** (1980) 971; W. Marciano and A. Sirlin, *Phys. Rev. D* **22** (1980) 2695.
 28. A. Freitas, W. Hollik, W. Walter and G. Weiglein, *Phys. Lett. B* **495** (2000) 338 [Erratum-ibid. **B 570** (2003) 260] [arXiv:hep-ph/0007091]; *Nucl. Phys. B* **632** (2002) 189 [Erratum-ibid. **B 666** (2003) 305] [arXiv:hep-ph/0202131]; M. Awramik and M. Czakon, *Phys. Lett. B* **568** (2003) 48, [arXiv:hep-ph/0305248].
 29. M. Awramik and M. Czakon, *Phys. Rev. Lett.* **89** (2002) 241801 [arXiv:hep-ph/0208113]; *Nucl. Phys. Proc. Suppl.* **116** (2003) 238 [arXiv:hep-ph/0211041]; A. Onishchenko and O. Veretin, *Phys. Lett. B* **551** (2003) 111 [arXiv:hep-ph/0209010]; M. Awramik, M. Czakon, A. Onishchenko and O. Veretin, *Phys. Rev. D* **68** (2003) 053004 [arXiv:hep-ph/0209084].
 30. A. Djouadi and C. Verzegnassi, *Phys. Lett. B* **195** (1987) 265; A. Djouadi, *Nuovo Cim. A* **100** (1988) 357.
 31. B. Kniehl, *Nucl. Phys. B* **347** (1990) 89; F. Halzen and B. Kniehl, *Nucl. Phys. B* **353** (1991) 567; B. Kniehl and A. Sirlin, *Nucl. Phys. B* **371** (1992) 141; *Phys. Rev. D* **47** (1993) 883; A. Djouadi and P. Gambino, *Phys. Rev. D* **49** (1994) 3499 [Erratum-ibid. **D 53** (1994) 4111] [arXiv:hep-ph/9309298].
 32. M. Awramik, M. Czakon, A. Freitas and G. Weiglein, *Phys. Rev. D* **69** (2004) 053006 [arXiv:hep-ph/0311148].
 33. L. Avdeev et al., *Phys. Lett. B* **336** (1994) 560 [Erratum-ibid. **B 349** (1995) 597] [arXiv:hep-ph/9406363]; K. Chetyrkin, J. Kühn and M. Steinhauser, *Phys. Lett. B* **351** (1995) 331 [arXiv:hep-ph/9502291]; *Nucl. Phys. B* **482** (1996) 213 [arXiv:hep-ph/9606230].
 34. K. Chetyrkin, J. Kühn and M. Steinhauser, *Phys. Rev. Lett.* **75** (1995) 3394 [arXiv:hep-ph/9504413].
 35. M. Veltman, *Nucl. Phys. B* **123** (1977) 89.
 36. J. van der Bij, K. Chetyrkin, M. Faisst, G. Jikia and T. Seidensticker, *Phys. Lett. B* **498** (2001) 156 [arXiv:hep-ph/0011373].
 37. M. Faisst, J. Kühn, T. Seidensticker and O. Veretin, *Nucl. Phys. B* **665** (2003) 649 [arXiv:hep-ph/0302275].
 38. R. Boughezal, J. Tausk and J. van der Bij, *Nucl. Phys. B* **713** (2005) 278 [arXiv:hep-ph/0410216].
 39. Y. Schröder and M. Steinhauser, *Phys. Lett. B* **622** (2005) 124 [arXiv:hep-ph/0504055]; K. Chetyrkin, M. Faisst, J. Kühn, P. Maierhofer and C. Sturm, *Phys. Rev. Lett.* **97** (2006) 102003 [arXiv:hep-ph/0605201]; R. Boughezal and M. Czakon, *Nucl. Phys. B* **755** (2006) 221 [arXiv:hep-ph/0606232].
 40. S. Heinemeyer, W. Hollik, D. Stöckinger, A.M. Weber and G. Weiglein, *JHEP* **08** (2006) 052 [arXiv:hep-ph/0604147].
 41. P. Chankowski, A. Dabelstein, W. Hollik, W. Möhle, S. Pokorski and J. Rosiek, *Nucl. Phys. B* **417** (1994) 101.
 42. D. Garcia and J. Solà, *Mod. Phys. Lett. A* **9** (1994) 211.
 43. A. Djouadi, P. Gambino, S. Heine-

- meyer, W. Hollik, C. Jünger and G. Weiglein, *Phys. Rev. Lett.* **78** (1997) 3626 [arXiv:hep-ph/9612363]; *Phys. Rev. D* **57** (1998) 4179 [arXiv:hep-ph/9710438].
44. S. Heinemeyer and G. Weiglein, *JHEP* **0210** (2002) 072 [arXiv:hep-ph/0209305]; arXiv:hep-ph/0301062.
45. J. Haestier, S. Heinemeyer, D. Stöckinger and G. Weiglein, *JHEP* **0512** (2005) 027 [arXiv:hep-ph/0508139]; arXiv:hep-ph/0506259.
46. LEP Higgs working group, *Phys. Lett. B* **565** (2003) 61 [arXiv:hep-ex/0306033].
47. S. Heinemeyer, W. Hollik and G. Weiglein, *Eur. Phys. J. C* **9** (1999) 343 [arXiv:hep-ph/9812472].
48. G. Degrandi, S. Heinemeyer, W. Hollik, P. Slavich and G. Weiglein, *Eur. Phys. J. C* **28** (2003) 133 [arXiv:hep-ph/0212020].
49. Tevatron Electroweak Working Group, hep-ex/0703034.
50. A. Czarnecki and W. Marciano, *Phys. Rev. D* **64** (2001) 013014 [arXiv:hep-ph/0102122].
51. M. Knecht, *Lect. Notes Phys.* **629** (2004) 37 [arXiv:hep-ph/0307239]; M. Passera, *Nucl. Phys. Proc. Suppl.* **155** (2006) 365 [arXiv:hep-ph/0509372].
52. D. Stöckinger, *J. Phys. G* **34** (2007) R45 [arXiv:hep-ph/0609168].
53. J. Miller, E. de Rafael and B. Roberts, arXiv:hep-ph/0703049.
54. F. Jegerlehner, arXiv:hep-ph/0703125.
55. T. Kinoshita and M. Nio, *Phys. Rev. D* **70** (2004) 113001 [arXiv:hep-ph/0402206]; *Phys. Rev. D* **73** (2006) 053007 [arXiv:hep-ph/0512330].
56. M. Passera, *Phys. Rev. D* **75** (2007) 013002 [arXiv:hep-ph/0606174].
57. K. Hagiwara, A. Martin, D. Nomura and T. Teubner, *Phys. Lett. B* **649** (2007) 173 [arXiv:hep-ph/0611102].
58. M. Davier, *Nucl. Phys. Proc. Suppl.* **169** (2007) 288 [arXiv:hep-ph/0701163].
59. M. Knecht and A. Nyffeler, *Phys. Rev. D* **65** (2002) 073034 [arXiv:hep-ph/0111058]; M. Knecht, A. Nyffeler, M. Perrottet and E. De Rafael, *Phys. Rev. Lett.* **88** (2002) 071802 [arXiv:hep-ph/0111059]; I. Blokland, A. Czarnecki and K. Melnikov, *Phys. Rev. Lett.* **88** (2002) 071803 [arXiv:hep-ph/0112117]; M. Ramsey-Musolf and M. Wise, *Phys. Rev. Lett.* **89** (2002) 041601 [arXiv:hep-ph/0201297]; J. Kühn, A. Onishchenko, A. Pivovarov and O. Veretin, *Phys. Rev. D* **68** (2003) 033018 [arXiv:hep-ph/0301151].
60. K. Melnikov and A. Vainshtein, *Phys. Rev. D* **70** (2004) 113006 [arXiv:hep-ph/0312226].
61. M. Davier and W. Marciano, *Ann. Rev. Nucl. Part. Sci.* **54** (2004) 115.
62. A. Aloisio et al. [KLOE Collaboration], *Phys. Lett. B* **606** (2005) 12 [arXiv:hep-ex/0407048]; D. Leone [KLOE Collaboration], *Nucl. Phys. Proc. Suppl.* **162** (2006) 95.
63. R. Akhmetshin et al. [CMD-2 Collaboration], *Phys. Lett. B* **578** (2004) 285 [arXiv:hep-ex/0308008]; arXiv:hep-ex/0610021.
64. M. Achasov et al. [SND Collaboration], *J. Exp. Theor. Phys.* **101** (2005) 1053 [arXiv:hep-ex/0506076].
65. S. Müller, talk given at the EPS07, Manchester, July 2007, see: agenda.hep.man.ac.uk/contribution/Display.py?contribId=36&sessionId=26&confId=70.
66. S. Eidelman, talk given at the ICHEP06, Moscow, July 2006, see: ichep06.jinr.ru/reports/333_6s1_9p30_Eidelman.pdf.
67. T. Moroi, *Phys. Rev. D* **53** (1996) 6565 [Erratum-ibid. **D 56** (1997) 4424] [arXiv:hep-ph/9512396].
68. S. Abel, W. Cottingham and I. Whittingham, *Phys. Lett. B* **259** (1991) 307; J. Lopez, D. Nanopoulos and X. Wang, *Phys. Rev. D* **49** (1994) 366, hep-ph/9308336.
69. G. Degrandi and G. Giudice, *Phys.*

- Rev. D* **58** (1998) 053007 [arXiv:hep-ph/9803384].
70. S. Heinemeyer, D. Stöckinger and G. Weiglein, *Nucl. Phys. B* **690** (2004) 62 [arXiv:hep-ph/0312264].
 71. S. Heinemeyer, D. Stöckinger and G. Weiglein, *Nucl. Phys. B* **699** (2004) 103 [arXiv:hep-ph/0405255].
 72. D. Hertzog, J. Miller, E. de Rafael, B. Lee Roberts and D. Stöckinger, arXiv:0705.4617 [hep-ph].
 73. K. Jungmann, arXiv:hep-ex/0703031.
 74. B. Regan, E. Commins, C. Schmidt and D. DeMille, *Phys. Rev. Lett.* **88** (2002) 071805.
 75. C. Baker et al., *Phys. Rev. Lett.* **97** (2006) 131801 [arXiv:hep-ex/0602020].
 76. M. Romalis, W. Griffith and E. Fortson, *Phys. Rev. Lett.* **86** (2001) 2505 [arXiv:hep-ex/0012001].
 77. M. Ramsey-Musolf and S. Su, arXiv:hep-ph/0612057.
 78. C. Jarlskog, *Phys. Rev. Lett.* **55** (1985) 1039.
 79. I. Khriplovich and S. Lamoreaux, “CP Violation Without Strangeness: Electric Dipole Moments Of Particles, Atoms, And Molecules” *Berlin, Germany: Springer (1997) 230 p*; J. Ginges and V. Flambaum, *Phys. Rept.* **397** (2004) 63 [arXiv:physics/0309054]; J. Erler and M. Ramsey-Musolf, *Prog. Part. Nucl. Phys.* **54** (2005) 351 [arXiv:hep-ph/0404291].
 80. W. Hollik, J. Illana, S. Rigolin and D. Stöckinger, *Phys. Lett. B* **416** (1998) 345 [arXiv:hep-ph/9707437]; *Phys. Lett. B* **425** (1998) 322 [arXiv:hep-ph/9711322].
 81. D. Demir, O. Lebedev, K. Olive, M. Pospelov and A. Ritz, *Nucl. Phys. B* **680** (2004) 339 [arXiv:hep-ph/0311314].
 82. D. Chang, W. Keung and A. Pilaftsis, *Phys. Rev. Lett.* **82** (1999) 900 [Erratum-ibid. **83** (1999) 3972] [arXiv:hep-ph/9811202]; A. Pilaftsis, *Phys. Lett. B* **471** (1999) 174 [arXiv:hep-ph/9909485].
 83. S. Abel, S. Khalil and O. Lebedev, *Nucl. Phys. B* **606** (2001) 151 [arXiv:hep-ph/0103320].
 84. M. Pospelov and A. Ritz, *Annals Phys.* **318** (2005) 119 [arXiv:hep-ph/0504231].
 85. J. Ellis, S. Ferrara and D. Nanopoulos, *Phys. Lett. B* **114** (1982) 231.
 86. T. Feng, X. Li, J. Maalampi and X. Zhang, *Phys. Rev. D* **71** (2005) 056005 [arXiv:hep-ph/0412147].
 87. P. Nath, *Phys. Rev. Lett.* **66** (1991) 2565; Y. Kizukuri and N. Oshimo, *Phys. Rev. D* **46** (1992) 3025.
 88. T. Ibrahim and P. Nath, *Phys. Lett. B* **418** (1998) 98 [arXiv:hep-ph/9707409]; *Phys. Rev. D* **57** (1998) 478 [Erratum-ibid. **58** (1998) 019901] [Erratum-ibid. **60** (1998) 079903] [Erratum-ibid. **60** (1999) 119901] [arXiv:hep-ph/9708456]; M. Brhlik, G. Good and G. Kane, *Phys. Rev. D* **59**, 115004 (1999) [arXiv:hep-ph/9810457].
 89. V. Barger, T. Falk, T. Han, J. Jiang, T. Li and T. Plehn, *Phys. Rev. D* **64** (2001) 056007 [arXiv:hep-ph/0101106].
 90. M. Grünewald, *priv. communication*.
 91. G. Montagna, O. Nicrosini, F. Piccinini and G. Passarino, *Comput. Phys. Commun.* **117** (1999) 278 [arXiv:hep-ph/9804211].
 92. D. Bardin et al., *Comput. Phys. Commun.* **133** (2001) 229 [arXiv:hep-ph/9908433]; A. Arbuzov et al., *Comput. Phys. Commun.* **174** (2006) 728 [arXiv:hep-ph/0507146].
 93. U. Baur, R. Clare, J. Erler, S. Heinemeyer, D. Wackeroth, G. Weiglein and D. Wood, arXiv:hep-ph/0111314.
 94. S. Heinemeyer, T. Mannel and G. Weiglein, arXiv:hep-ph/9909538; J. Erler, S. Heinemeyer, W. Hollik, G. Weiglein and P. Zerwas, *Phys. Lett. B* **486** (2000) 125 [arXiv:hep-ph/0005024]; J. Erler and S. Heinemeyer, arXiv:hep-ph/0102083.
 95. R. Hawkins and K. Mönig, *EPJdirect* **C8** (1999) 1 [arXiv:hep-ex/9910022].
 96. G. Wilson, LC-PHSM-2001-009, see:

- www.desy.de/~lcnotes/notes.html.
97. S. Heinemeyer, W. Hollik, A.M. Weber and G. Weiglein, arXiv:0710.2972 [hep-ph].
 98. H. Haber and R. Hempfling, *Phys. Rev. Lett.* **66** (1991) 1815; Y. Okada, M. Yamaguchi and T. Yanagida, *Prog. Theor. Phys.* **85** (1991) 1; J. Ellis, G. Ridolfi and F. Zwirner, *Phys. Lett. B* **257** (1991) 83; *Phys. Lett. B* **262** (1991) 477; R. Barbieri and M. Frigeni, *Phys. Lett. B* **258** (1991) 395.
 99. M. Frank, T. Hahn, S. Heinemeyer, W. Hollik, H. Rzehak and G. Weiglein, *JHEP* **0702** (2007) 047 [arXiv:hep-ph/0611326].
 100. S. Heinemeyer, W. Hollik, H. Rzehak and G. Weiglein, to appear in *Phys. Lett. B*, arXiv:0705.0746 [hep-ph].
 101. A. Brignole, *Phys. Lett. B* **281** (1992) 284.
 102. P. Chankowski, S. Pokorski and J. Rosiek, *Phys. Lett. B* **286** (1992) 307; *Nucl. Phys. B* **423** (1994) 437 [arXiv:hep-ph/9303309].
 103. A. Dabelstein, *Nucl. Phys. B* **456** (1995) 25 [arXiv:hep-ph/9503443]; *Z. Phys. C* **67** (1995) 495 [arXiv:hep-ph/9409375].
 104. S. Heinemeyer, W. Hollik and G. Weiglein, *Phys. Rev. D* **58** (1998) 091701 [arXiv:hep-ph/9803277]; *Phys. Lett. B* **440** (1998) 296, [arXiv:hep-ph/9807423].
 105. S. Heinemeyer, W. Hollik and G. Weiglein, *Phys. Lett. B* **455** (1999) 179 [arXiv:hep-ph/9903404].
 106. S. Heinemeyer, W. Hollik, H. Rzehak and G. Weiglein, *Eur. Phys. J. C* **39** (2005) 465 [arXiv:hep-ph/0411114].
 107. M. Carena, H. Haber, S. Heinemeyer, W. Hollik, C. Wagner and G. Weiglein, *Nucl. Phys. B* **580** (2000) 29 [arXiv:hep-ph/0001002].
 108. R. Zhang, *Phys. Lett. B* **447** (1999) 89 [arXiv:hep-ph/9808299]; J. Espinosa and R. Zhang, *JHEP* **0003** (2000) 026 [arXiv:hep-ph/9912236]; *Nucl. Phys. B* **586** (2000) 3, [arXiv:hep-ph/0003246]; J. Espinosa and I. Navarro, *Nucl. Phys. B* **615** (2001) 82 [arXiv:hep-ph/0104047].
 109. G. Degrassi, P. Slavich and F. Zwirner, *Nucl. Phys. B* **611** (2001) 403 [arXiv:hep-ph/0105096]; A. Brignole, G. Degrassi, P. Slavich and F. Zwirner, *Nucl. Phys. B* **631** (2002) 195 [arXiv:hep-ph/0112177]; *Nucl. Phys. B* **643** (2002) 79, [arXiv:hep-ph/0206101]; G. Degrassi, A. Dedes and P. Slavich, *Nucl. Phys. B* **672** (2003) 144, [arXiv:hep-ph/0305127].
 110. M. Carena, J. Espinosa, M. Quirós and C. Wagner, *Phys. Lett. B* **355** (1995) 209, [arXiv:hep-ph/9504316]; M. Carena, M. Quirós and C. Wagner, *Nucl. Phys. B* **461** (1996) 407 [arXiv:hep-ph/9508343]; J. Casas, J. Espinosa, M. Quirós and A. Riotto, *Nucl. Phys. B* **436** (1995) 3, [Erratum-ibid. **B** **439** (1995) 466] [arXiv:hep-ph/9407389].
 111. M. Carena, D. Garcia, U. Nierste and C. Wagner, *Nucl. Phys. B* **577** (2000) 577 [arXiv:hep-ph/9912516].
 112. H. Eberl, K. Hidaka, S. Kraml, W. Majerotto and Y. Yamada, *Phys. Rev. D* **62** (2000) 055006 [arXiv:hep-ph/9912463]; J. Guasch, P. Häfliger and M. Spira, *Phys. Rev. D* **68** (2003) 115001 [arXiv:hep-ph/0305101].
 113. B. Allanach, A. Djouadi, J. Kneur, W. Porod and P. Slavich, *JHEP* **0409** (2004) 044 [arXiv:hep-ph/0406166].
 114. S. Heinemeyer, W. Hollik and G. Weiglein, *Comput. Phys. Commun.* **124** (2000) 76 [arXiv:hep-ph/9812320]; see: www.feynhiggs.de.
 115. J. Lee, A. Pilaftsis et al., *Comput. Phys. Commun.* **156** (2004) 283 [arXiv:hep-ph/0307377].
 116. S. Martin, *Phys. Rev. D* **65** (2002) 116003 [arXiv:hep-ph/0111209]; *Phys. Rev. D* **66** (2002) 096001 [arXiv:hep-ph/0206136]; *Phys. Rev. D* **67** (2003) 095012 [arXiv:hep-ph/0211366]; *Phys. Rev. D* **68** 075002 (2003) [arXiv:hep-ph/0307101]; *Phys. Rev. D* **70** (2004)

- 016005 [arXiv:hep-ph/0312092]; *Phys. Rev. D* **71** (2005) 016012 [arXiv:hep-ph/0405022]; *Phys. Rev. D* **71** (2005) 116004 [arXiv:hep-ph/0502168]; *Phys. Rev. D* **75** (2007) 055005 [arXiv:hep-ph/0701051]; S. Martin and D. Robertson, *Comput. Phys. Commun.* **174** (2006) 133 [arXiv:hep-ph/0501132].
117. S. Heinemeyer, S. Kraml, W. Porod and G. Weiglein, *JHEP* **0309** (2003) 075 [arXiv:hep-ph/0306181].
118. S. Heinemeyer, W. Hollik and G. Weiglein, *JHEP* **0006** (2000) 009 [arXiv:hep-ph/9909540].
119. J. Ellis, S. Heinemeyer, K. Olive, A.M. Weber and G. Weiglein, *JHEP* **0708** (2007) 083 [arXiv:0706.0652 [hep-ph]].
120. C. Bennett et al., *Astrophys. J. Suppl.* **148** (2003) 1 [arXiv:astro-ph/0302207]; D. Spergel et al. [WMAP Collaboration], *Astrophys. J. Suppl.* **148** (2003) 175 [arXiv:astro-ph/0302209]; *Astrophys. J. Suppl.* **170** (2007) 377 [arXiv:astro-ph/0603449].
121. J. Ellis, K. Olive, Y. Santoso and V. Spanos, *Phys. Lett. B* **565** (2003) 176 [arXiv:hep-ph/0303043].
122. U. Chattopadhyay, A. Corsetti and P. Nath, *Phys. Rev. D* **68** (2003) 035005 [arXiv:hep-ph/0303201]; H. Baer and C. Balazs, *JCAP* **0305** (2003) 006 [arXiv:hep-ph/0303114]; A. Lahanas and D. Nanopoulos, *Phys. Lett. B* **568** (2003) 55 [arXiv:hep-ph/0303130]; R. Arnowitt, B. Dutta and B. Hu, arXiv:hep-ph/0310103.
123. S. Ambrosanio, A. Dedes, S. Heinemeyer, S. Su and G. Weiglein, *Nucl. Phys. B* **624** (2001) 3 [arXiv:hep-ph/0106255].
124. J. Ellis, S. Heinemeyer, K. Olive and G. Weiglein, *Phys. Lett. B* **515** (2001) 348 [arXiv:hep-ph/0105061].
125. J. Ellis, S. Heinemeyer, K. Olive and G. Weiglein, *JHEP* **0502** 013 [arXiv:hep-ph/0411216]; arXiv:hep-ph/0508169.
126. J. Ellis, S. Heinemeyer, K. Olive and G. Weiglein, *JHEP* **0605** (2006) 005 [arXiv:hep-ph/0602220].
127. B. Allanach and C. Lester, *Phys. Rev. D* **73** (2006) 015013 [arXiv:hep-ph/0507283]; B. Allanach, C. Lester, and A.M. Weber, *JHEP* **12** (2006) 065 [arXiv:hep-ph/0609295]; C. Allanach, K. Cranmer, C. Lester, and A.M. Weber, arXiv:0705.0487 [hep-ph].
128. O. Buchmüller et al., to appear in *Phys. Lett. B*, arXiv:0707.3447 [hep-ph].
129. R. de Austri, R. Trotta and L. Roszkowski, *JHEP* **0605** (2006) 002 [arXiv:hep-ph/0602028]; *JHEP* **0704** (2007) 084 [arXiv:hep-ph/0611173]; *JHEP* **0707** (2007) 075 [arXiv:0705.2012 [hep-ph]].
130. G. Isidori, F. Mescia, P. Paradisi and D. Temes, *Phys. Rev. D* **75** (2007) 115019 [arXiv:hep-ph/0703035]; M. Carena, A. Menon and C. Wagner, *Phys. Rev. D* **76** (2007) 035004 [arXiv:0704.1143 [hep-ph]].
131. A. Dedes, S. Heinemeyer, S. Su and G. Weiglein, *Nucl. Phys. B* **674** (2003) 271 [arXiv:hep-ph/0302174].
132. LEP Higgs working group, *Eur. Phys. J. C* **47** (2006) 547 [arXiv:hep-ex/0602042].
133. M. Awramik, M. Czakon, A. Freitas and G. Weiglein, *Phys. Rev. Lett.* **93** (2004) 201805 [arXiv:hep-ph/0407317].